



# Determining the role of lineaments in underground hydrodynamics using Landsat 7 ETM+ data, case of the Chott El Gharbi Basin (western Algeria)

Mebarka Takorabt<sup>1</sup> · Ahmed Cherif Toubal<sup>1</sup> · Hamid Haddoum<sup>1</sup> · Siham Zerrouk<sup>1</sup>

Received: 12 July 2017 / Accepted: 25 January 2018  
© The Author(s) 2018. This article is an open access publication

## Abstract

This paper attempts an overview of the application of remote sensing to groundwater studies. Its objective is to define the role of the geological features in the underground hydrodynamic in the aquifer system of the Chott El Gharbi Basin (Algerian western high plains) and identify a link between the fracturing and the meteoric water supply of this deep aquifer. The methodology followed consists to study the fracturing map of studied area which is obtained after Landsat 7 ETM+ processing images. It is based on structural lineaments mapping. The obtained map has been validated by geophysical results and geological map. Statistical analysis of the lineaments network shows the presence of about 537 lineaments divided into four families oriented according to the following directions NE-SW, NW-SE, N-S, and E-W. The lineament analysis of the studied basin provides important information on subsurface fractures that may control the circulation and storage of groundwater. These fractures have an undeniable hydrogeological interest because of their size, a priori favorable for the aquifers recharge in the region. The probable link between the Chott El Gharbi implementation and the presence of mega fractures which some of them correspond actually to Wadis is confirmed. The correlation between the productivity of high debit drillings and the closest lineament confirms that these lineaments are surface traces of regional discontinuities and act as main groundwater flow paths.

**Keywords** Chott El Gharbi Basin · Landsat 7 ETM+ · Lineaments · Geophysical methods · Groundwater flow

## Introduction

The exploitation of the groundwater in the dry areas in Algeria involves one of the main sources of the drinkable water supply. In order to reply to the durable needs of the populations, the good knowledge of this vital resource is a need to ensure its good management.

The study area is situated in the extreme west of the high Oranian western plains in Algeria, more exactly the Chott El Gharbi Basin. This area is the seat of vast aquifers system multilayers bordered by two major structures (Tlemcen Mountains in the North and Djebel Ksour in the South). In spite of the major importance of the groundwater resources in

this system, the hydrodynamic characteristics of the aquifers are little-known.

This study demonstrates the use of LANDSAT 7 ETM+ (Enhanced Thematic Mapper Plus) imagery data for mapping and analyses of lineaments in study area. Its objective is to illustrate the application of these techniques for the structural and hydrogeological characterization.

The main purpose is to define the structural context of the borders, and the center of the basin, and to establish a link between the fracturing and the water supply of the deep aquifers, thus to understand its role in the hydrodynamic functioning of this hydrogeological system. In fact, this work required the coupled use of remote sensing and geophysics data. The remote sensing technics constitute a reliable approach in the detection and the mapping of fractures (Kouassi et al. 2014; Ndong et al. 2014). Generally, the Geophysical methods and especially, the electric prospecting allow specifying the location and the depth of the tectonic discontinuities susceptible to be a seat of the groundwater circulation. Indeed, they allow determining with a better precision the positioning of hydrogeological interest zones

---

✉ Mebarka Takorabt  
takorabetmebarka@hotmail.fr

<sup>1</sup> FSTGAT, Université des Sciences et de la Technologie Houari Boumediene, B.P. 32, USTHB, 16123, Bab-Ezzouar, Alger, Algeria

(Israel et al. 1996; Thomas et al. 2002; Vouillamoz et al. 2003; Boutaleb et al. 2009; Sombo et al. 2011; Kouassi et al. 2014).

More than half century ago, the use of the satellite imaging is recommended as the best way for the hydrogeological prospecting studies, to identify accumulation and transfer of groundwater zones (Jourda et al. 2005, 2006; Amadi and Olasehinde, 2010). Numerous studies (Kresic 1994; Youan et al. 2009; Boutaleb et al. 2009; Mahamadou et al. 2010) showed that the satellite images contribute to the detection of the geological features that have a direct link with the groundwater flow. These various works collaborated in the recognition of the lineaments' importance for the hydrogeology (Youan et al. 2009), then application of remote sensing to efficient groundwater resource exploration and management (Mogaji et al. 2011).

The methodology followed in this work includes the processing, interpreting of the Landsat-7 ETM+ satellite images, establishing a structural map from these images, and detecting the geological faults which can drain infiltrated waters (Boutaleb et al. 2009). The qualitative and quantitative analyses of the lineaments map covering the studied basin after its validation by the electric prospecting results allow to confirm the existence of these structural elements and to specify their characteristics in depth (Kouassi et al. 2014). Finally, this work allows to show the role of lineaments in the alimentation of the aquifer system of the study area, and to analyze the general structural behavior of the region through a statistical study of the identified lineaments.

## Study area

### General setting of study area

The Chott El Gharbi watershed is located in the western part of the High Oranian Plains (west of Algeria) (Fig. 1). It is characterized by a semi-arid to arid climate with irregular and low pluviometry (100 at 300 mm/year (Benabadji and Bouazza 2000a, b). The relief is almost flat, except in the central part where the Chott is dominated by the cliffs cut of 40 to 50 m height. The bordering basin in the north and in the south that constitute the Tlemcen mounts and Saharan Atlas shows the summits that exceed sometimes 1600 m height (Djebaili et al. 1984; Azzaz 1996).

### Geologic and hydrogeologic setting

Geologically (Fig. 2), this region is formed by a Paleozoic basement composed of Shale, sometimes metamorphosed. Ordovician to carboniferous fossiliferous limestones, and Sandstones (Benzaquen 1965; Boutaleb et al. 2009), appear to favor breaks (this formation is flush with faults (tectonics) (Halitim 1988). These deposits are surmounted by a Triassic series, represented by Gypsum clays and red

Salts, purples or multicolored appearing abruptly within more recent layer following diapiric phenomena. This Triassic appears much localized in some points and in depressions level (Auclair and Biehler 1967). The Jurassic includes Dolomites on the base, Lias limestones and Marl-Limestones supporting Sandstone and multicolored Clays, (Jurassic passage to the Cretaceous), and ends by Dogger carbonate slab; it occupies the high plain reliefs such as the Djebel Antar, the Djebel Amrag, and Djebel Hafid. The end of the Jurassic to the Albian is marked by formation of the Sandstone sediment layer (Benest 1985; Azzaz 1986, 1996).

The Cenomanian shows Marl and Marl-Calcareous facies with thickness of less than 100 m. The marine series of the Cretaceous end by powerful Turonian Calcareous benches which thickness can exceed 150 m. The Senonian begins with Conglomerates which succeed clays; it ends by Gypsum benches. The Quaternary is constituted by the recent Alluviums that occupy the depressions and the valleys bottoms. It is represented by sediments covered by fragment of rocks, with alluviums, limestones, and wind contributions (Azzaz 1986, 1996).

The geological structure in the Algerian western high plains is formed by the big longitudinal and SW-NE faults. The geological study of the basin highlights a synclorium structure affected by two big faults (the North Atlassic fault and the South Atlassic fault) (Auclair and Biehler 1967). In the sedimentary covering, the major and secondary faults are distinguished. The N-E faults predominate; the N-W directions and meridional faults are less developed. According to these faults, some tectonic movements are repeated several times during the Triassic and Jurassic tectonic activation (Benest 1985). The geophysical data confirmed the rooting of several faults in the Paleozoic basement. The E-W longitudinal faults affecting the deep features Cretaceous and Jurassic are also highlighted by the geophysical studies (Geological and Mining Research Office) (Office de Recherche Géologiques et Minières (ORGM) 2006).

In the Tertiary, these zones underwent big tectonic movements represented by three compression phases of NNE-SSW to N-S directions and two distension (SW-NE) phases. From where the appearance of the flexible structures represented by upwarping, and depressions, and breakable structures marked by NE-SW, NW-SE, and ENE-WSW directions fault (Benest 1985), these tectonic phases are the following:

1. Pyreneo-Atlassic compressive phase: It is the major phase in the Saharan Atlas and a big part of the Maghreb. The compression was of axis 150° N to 180° E, and numerous faults played in strike-slip (Guardia 1970).
2. Last Eocene-Oligocene distension phase: This phase is largely evoked by the authors (Guardia 1970; Benest 1982, 1985; Delteil et al. 1971 in Bensalah

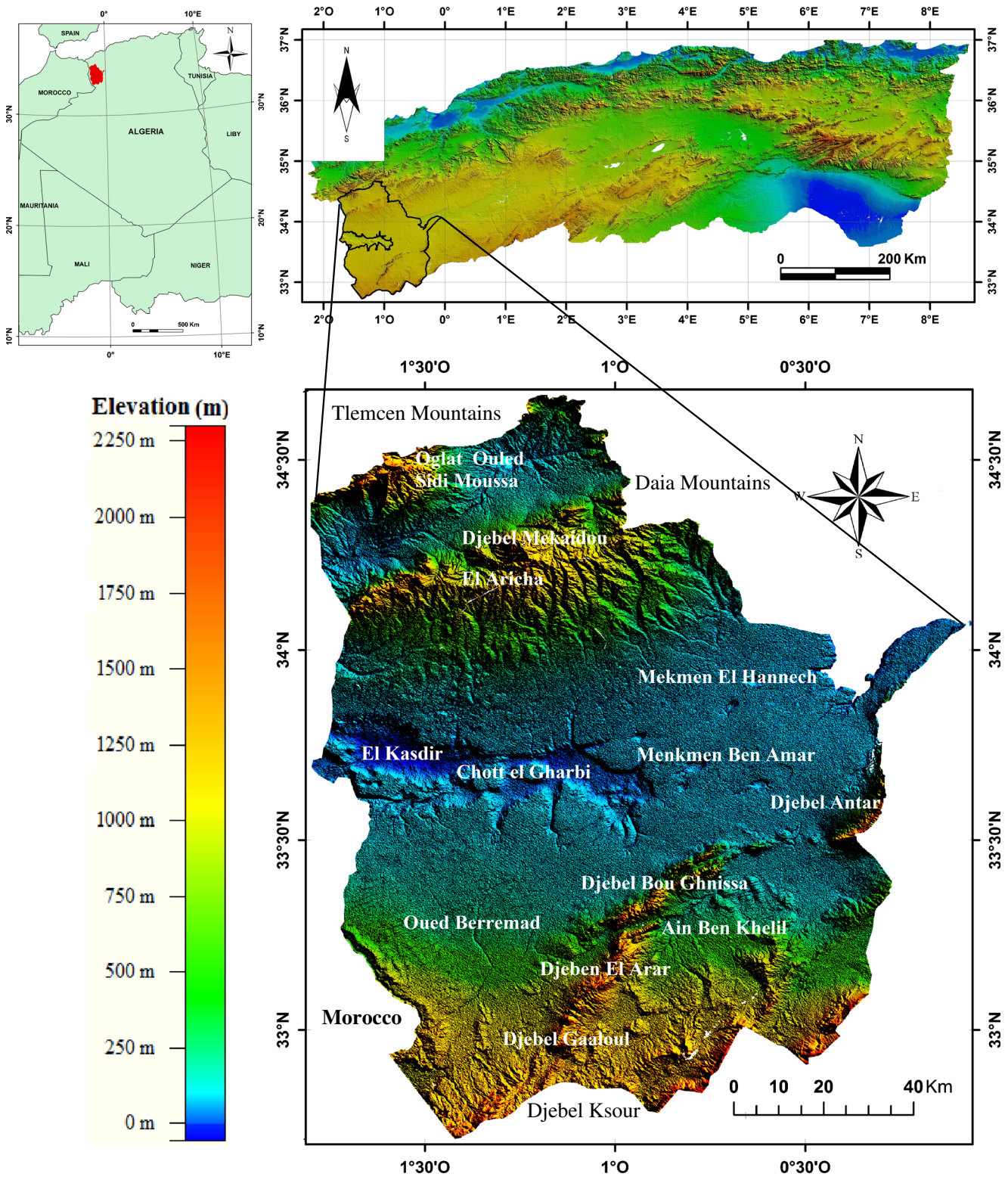


Fig. 1 Location map of study area

et al. 2005). It is responsible of reactivation of the old fault in the basement according to 55°–80° N and 140° N oriented faults. The forming of 60° NE horst and graben structures is associated to this phase.

Giving rise to NE-SW faults. This movement of the faults seems to precede the uprising of the Tlemcen Mounts during the following compressive phase, in the Tell and in the High Plains.

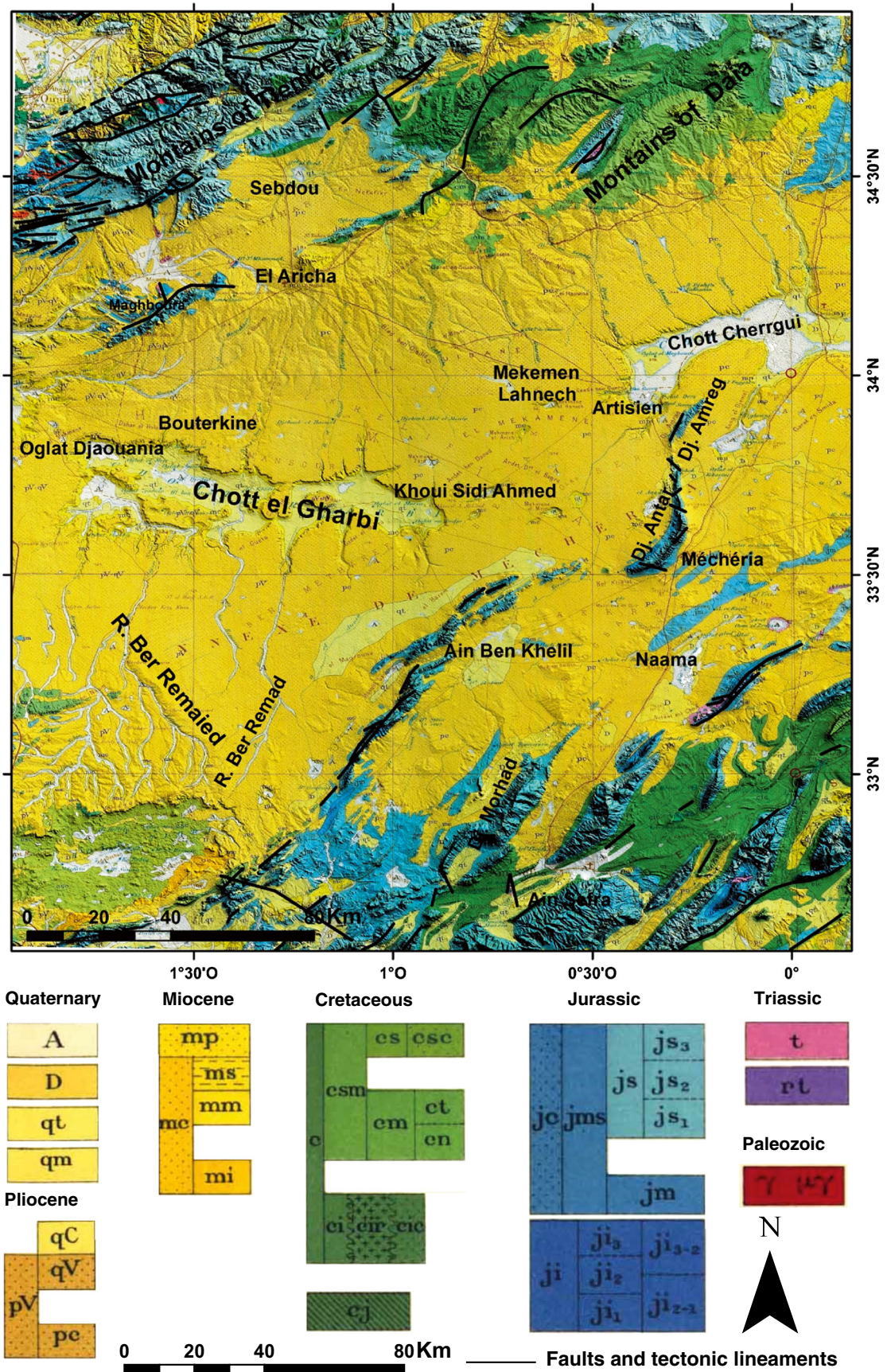


Fig. 2 Modified geological map of Algerian western high plains extracted from the geological map of Algeria at scale 1/500000>

3. Tortonian compression phase: This phase is responsible of the thrusting and implementation of small folds between rigid horsts (Guardia 1970; Delteil et al. 1971).
4. Distension phase between the Messenian and the Lower Quaternary: It was an important event in the Oranian with the forming of big subsiding basins. Certainly, it emphasizes the pre-existing horsts and the grabens (50° to 70° NE) (Benest 1985).
5. Quaternary and Neotectonic compression phase: This compression had to exacerbate the effects of the Tortonian phases (Benest 1985).

On hydrogeological view, three principal aquifers are distinguished:

- The Lacustrine Calcareous of the Neogene is cross cut in depths (between 4 and 200 m), is very cracked and distorted, and often owns a good permeability. Their alimentation is made initially by the outcrops, then through the faults which affect the deep features, or by drainage (Azzaz 1996).
- Sandstone Middle Cretaceous aquifer (Albian) consists of continental tab Sandstones in which the thickness is between 150 and 200 m in the Chott and changes between 50 and 100 m in the south (Saharan Atlas).
- The Jurassic aquifer constituted by Dolomites and Lacustrine Limestone, whose thickness is between 100 and 200 m, constitutes a karstic-type aquifer. This aquifer presents generally a fracture network, joints, and interconnected alteration zones, which confer it a high permeability (Azzaz 1986, 1996). On the tectonic plan, all the aquifer layers are affected by various direction faults.

## Hydrological setting

### Drainage system

The drainage network and catchment of the Chott El Gharbi were extracted from DEM (Digital Elevation Model) data and on screen digitization from topographic map (Fig. 3a, b). This watershed is drained by little-developed hydrographic network, whose total length is 19,034 km represented by 15 main wadis exceeding 6 km length. The permanent wadis are absent. Most of these rivers located in the north originate in the crests of the Tellian Atlas and flow to the south in the Chott. Other less importance rivers located in the south are characterized by a temporary flow. They originate at the northern flank of the Saharan Atlas located to the south and flow towards the north. The drainage system of this study area presents an incontestable adaptation to the tectonics in the region (Djebaili 1984).

The Chott is supplied with runoff water by a large endorheic hydrographic network (hydrography of the closed basin). All these wadis are in contact with salty rocks more or less furniture and contribute to the feeding and salting of groundwater.

### Drainage density (Dd)

The drainage density can indirectly indicate the groundwater potential of an area, due to its relation with surface runoff and permeability. It is defined as the total length of streams of all orders per drainage area (Horton 1932).

In the study area, drainage density has been identified and mapped as shown in Fig. 3c. This map shows that very high drainage density is found scattered in the southern, northern, and western parts. Moderate and low drainage density concentrates in the central and eastern parts.

## Data and methods

### Data

The main data used for the mapping of the structural lineaments is Landsat 7 ETM+ satellite images acquired on November 2001 corresponding to the dry season in the area (Path 198 row 36 and Path 198 row 37), downloaded from United States Geological Survey (USGS) web site. In addition to these data, several types of data were used; they include the geological map of the study area, extracted from the geological map of Algeria at 1/500,000 scale, and the topographic maps at 1/200,000 scale (topographic maps of Chott El Gharbi, Tlemcen, and Beni Ounif). These maps were provided by the National Institute of Mapping and Remote Sensing.

Finally, the results of two electrical prospecting companions realized in 1974 by the General Geophysical Company (Compagnie Générale de Géophysique CGG), then in 2006 by Geological and Mining Research Office (Office Nationale de Recherche Géologique et Minière ORGM), have also been used to correlate our results with.

### Methodology

The methodology followed in this present study is illustrated in Fig. 4. It includes two stages:

- The first stage consists of using the remote sensing to detect the present lineaments in the study area and then to identify the dominant families through statistical approach.
- The second stage consists of interpretation of lineament map, in order to determine the link between the fracturing and its probable role in the formation of the Chott El Gharbi hydrogeological basin, as well as the alimentation of its aquifers.

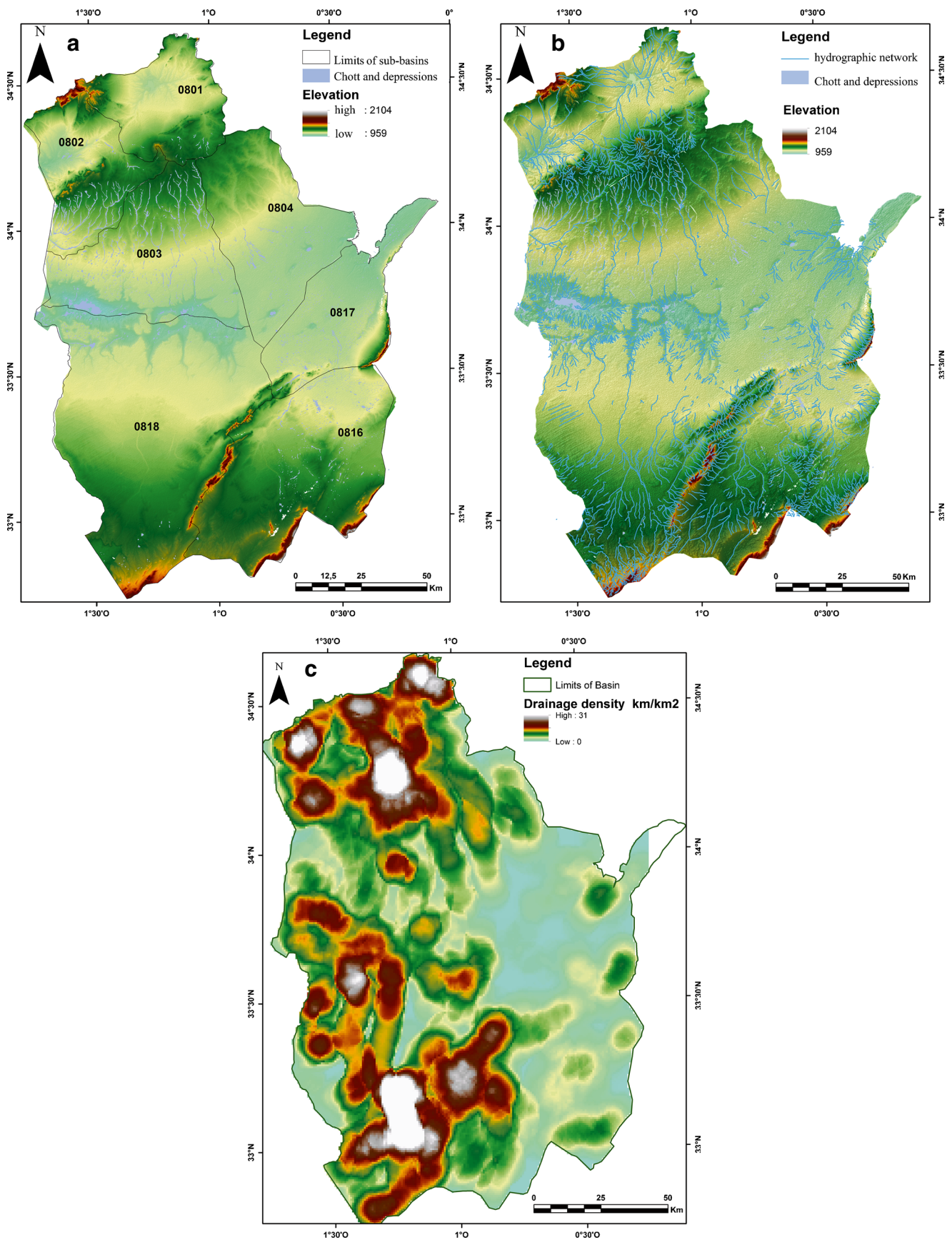


**Fig. 3** a The watershed of Chott El Gharbi Basin. b Drainage network of Chott El Gharbi catchment. c Drainage density map of Chott El Gharbi catchment

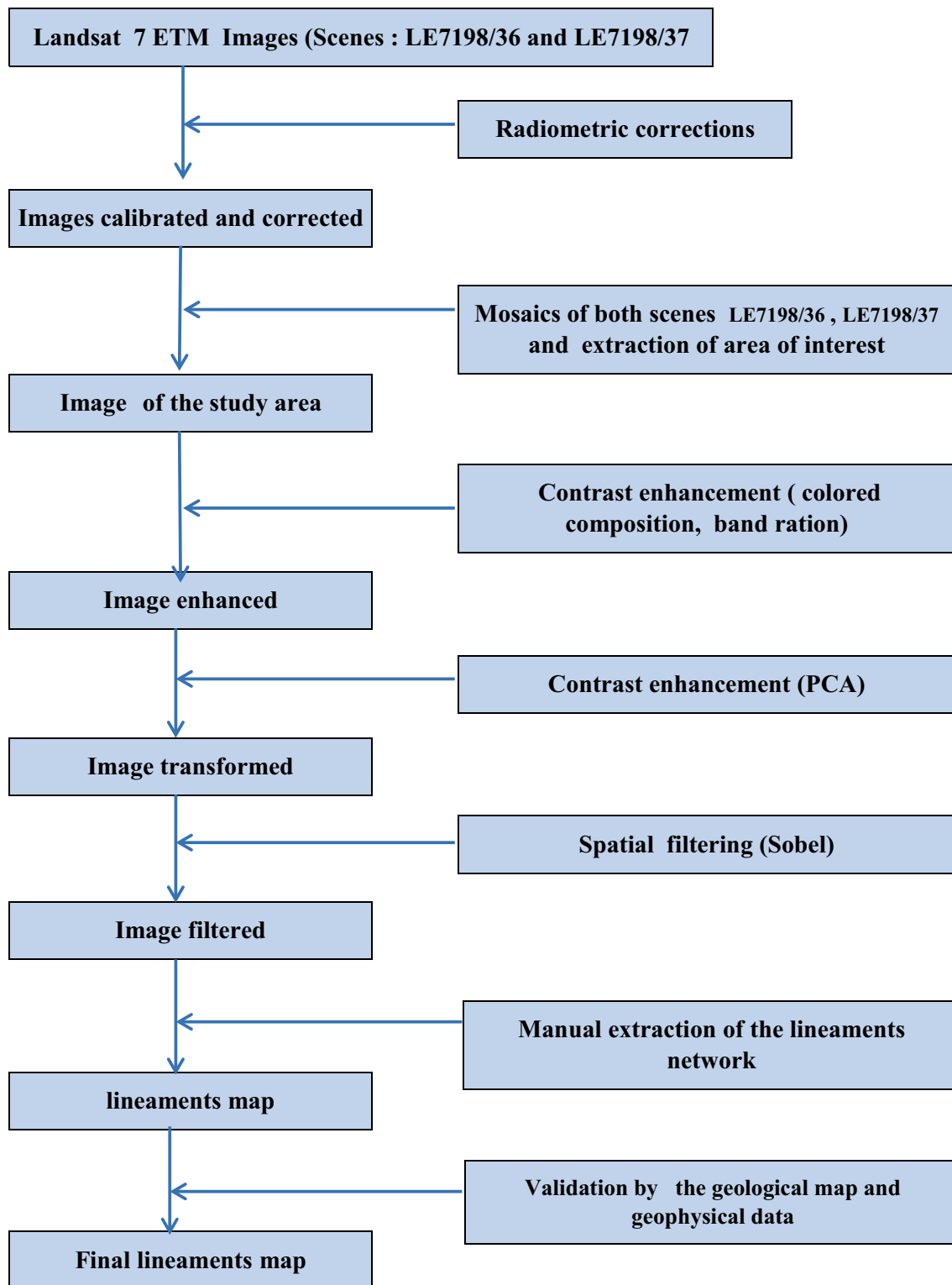


Fig. 4 Flowchart showing the methodology used in the present study

To judge the efficiency of the method used, the extracted lineaments from digital processing of satellite images have been confronted with geophysical results and geological data of preceded author’s works.

#### Digital processing of the Landsat 7 ETM+ images

The lineament extraction from the satellite images is based on image enhancement process in particular through their

radiometric correction (Boutaleb et al. 2009; Koita et al. 2010). In order to map the majority of the fractures affecting the study area, diverse digital processing techniques are then applied to better identify the wanted lineaments. These techniques include the colored compositions, the combinations of bands, the principal component analysis (PCA), and finally the directional filtering (Kassou et al. 2012).

To note, the band combination 341 (Fig. 5a) allows to obtain more readable and contrasted images. Besides, the calculation of the bands ratio, by taking least correlable bands, allowed realizing new colored compositions of the images (Boutaleb et al. 2009; Youan et al. 2009; Kouassi et al. 2014). According to some authors (Kouamé et al. 1999; Koita et al. 2010), the combinations that give best results are (ETM+4 + ETM+6), (ETM+7 + ETM+6), and the band ratio  $(ETM+6 - ETM+7)/(ETM+6 + ETM+7)$ , as well as combinations,  $ETM+5/ETM+4$ ,  $(ETM+6 + ETM+4)/(ETM+6 + ETM+4)$  (Youan et al. 2009).

The band ratio  $ETM+7 - ETM+4/ETM+7 + ETM+4$  allows visualizing the connected lineaments with the river system highlighting the flowing zones that are very important in hydrogeology (N'guessan et al. 2015). The  $(ETM+6 + ETM+4)$ ,  $(ETM+6 - ETM+4)/ETM+6 + ETM+4$ ,  $ETM+5/ETM+4$ , and  $(ETM+6 - ETM+7)/(ETM+6 + ETM+7)$  combinations, were used as input images for the filtering technics, which is a relevant processing for the enhancement of the linear structures (Youan et al. 2009).

The principal components analysis PCA is an effective technic to enhance the appearance of the multi-spectral images for geologic interpretation (Biémi 1991; Gannouni and Gabtni 2015; N'guessan et al. 2015). The application of this technic allowed us to create colored composition with the first three components. The filtering technic aims to eliminate the noise contained in the images. The directional filters improve the visualizing of the lineaments, by causing an optical shadow effect focused on the image as if it were illuminated by a raking light (Marion 1987; Gannouni and Gabtni 2015). The Sobel filter has the particularity enhancing the lineaments which are perpendicular to their direction (Coulibaly 1996). In this study, the applied filters are the Sobel filter following various directions  $0^\circ$ ,  $45^\circ$ ,  $90^\circ$ , and  $135^\circ$ . These filters were applied to the images derived from PCA analysis, as well as from the band ratio. These filters allow highlighting large of faults families according to different directions (Boutaleb et al. 2009; Youan et al. 2009, 2014; Koita et al. 2010; Kouassi et al. 2014; N'guessan et al. 2015).

### Structural mapping from the processing images

The structural lineament mapping consists to scan in the geographical information system (GIS) any linear structure observed on the processing images. This digitalization is based on the direct tracing of lineaments detected according to

various directions of filters. These images are superposed on the georeferenced topographic maps, to avoid a possible confusion of lineaments with the river system, and other anthropogenic activities (Kouamé et al. 1999; Lasm et al. 2004; Koita et al. 2010; Kassou et al. 2012; N'guessan et al. 2015).

The constitution of the fracture network allowed us, finally, to draw the map of structural element synthesis by superimposition of the different maps drawn according to different directions of the filters (Boutaleb et al. 2009).

The resulting map was obtained after the confrontation of the detected lineament network, with the data found on the existing geologic map (N'guessan et al. 2015), the geophysical campaign results, and the works of the different authors.

## Results and discussions

### Results of the Landsat 7 ETM+ processing

The principal component 1 (PC1) image (Fig. 5b) shows 81% of the variance. This component contains the maximum of information (the lineaments that are more visible in the PCA1 than in the raw image). The principal component 2 (PC2) image did not contain linear objects, even after the processing. Thus, the use of the PC1 image as working image is a justifiable choice. The RGB (*Red, Green and Blue*) image resulted from the colored composition (PC1, PC2, and PC3) (Fig. 5c) and allows the lithological discrimination between the features (Youan et al. 2009, 2014; Koita et al. 2010). So, the Jurassic seems green and blue. The Quaternary features appear in purple, pink, greenish yellow, and pink.

The calculation of the bands ratio allowed realizing new colored compositions. In the case of this study, the composition which gave the best result is  $(ETM+6 + ETM+4)$ ,  $(ETM+6 - ETM+4)/(ETM+6 + ETM+4)$ ,  $ETM+5/ETM+4$  (Fig. 5d) (Youan et al. 2009, 2014). On the image of this composite, the Jurassic appears in purple and blue, and the Quaternary is green.

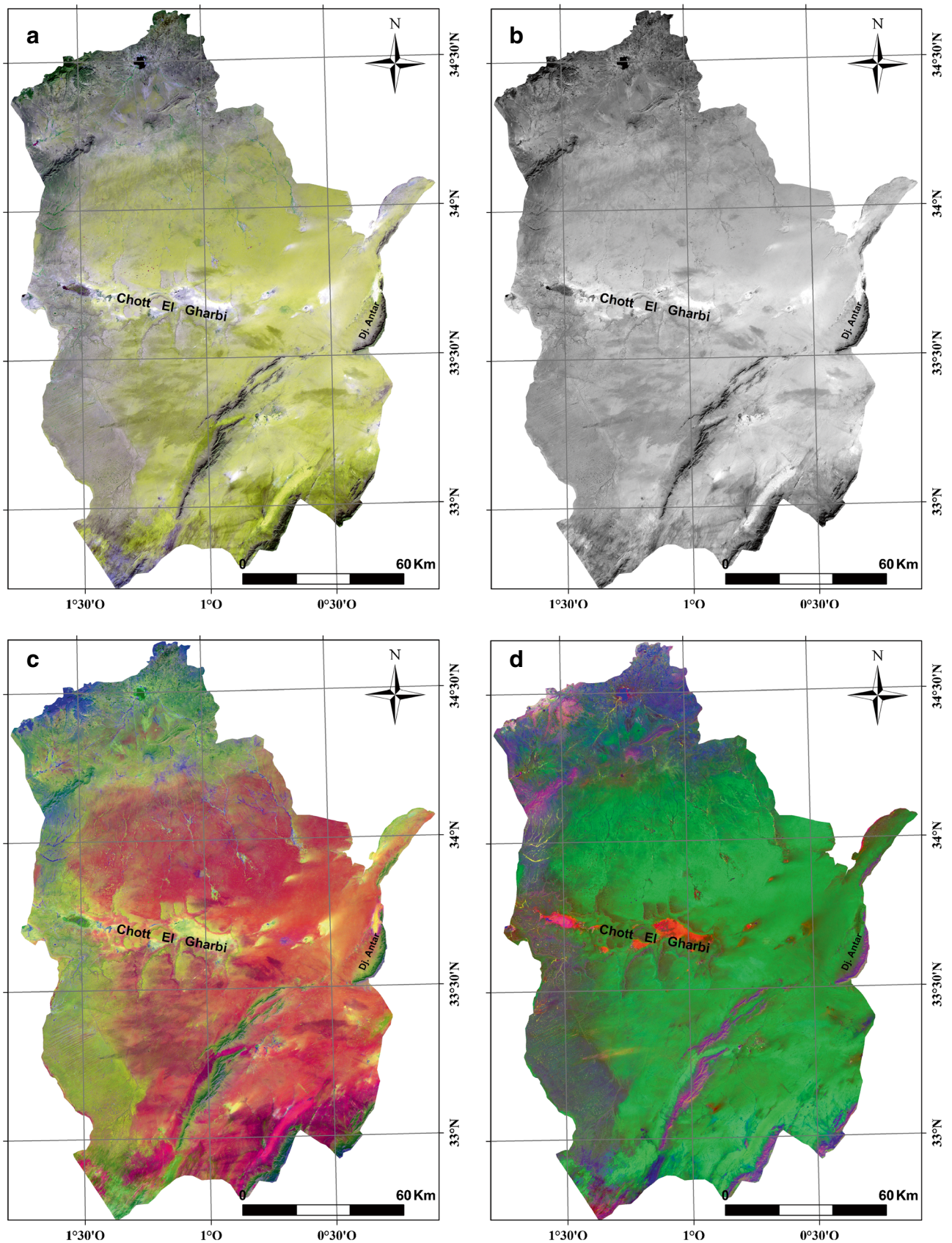
Most of the information (at least 80%) is observed in PC1. So, the application of the filtering to this first principal component is chosen. To maximize the extraction of lineaments in all directions, the Sobel directional filters in the directions  $0^\circ$ ,  $45^\circ$ ,  $90^\circ$ , and  $135^\circ$  are applied to this image.

Figure 6 shows the product of each of these filters. The Sobel filter images outlined the various features and the mega tectonic faults which affect them (Youan et al. 2009, 2014).

### Orientation of the lineaments networks

The fracture network analysis of this region obtained after the diverse treatments of the image Landsat TM proves the existence of the dominant orientations of lineaments. The final lineament networks map (Fig. 7a) shows four main directions





**Fig. 5** a True color combination: RGB 341. b Principal component 1 PC1. c Color combination of principal component analysis PCA123. d Color combination of Band Ratio 6 + 4, 6-4/6 + 4, 5/4

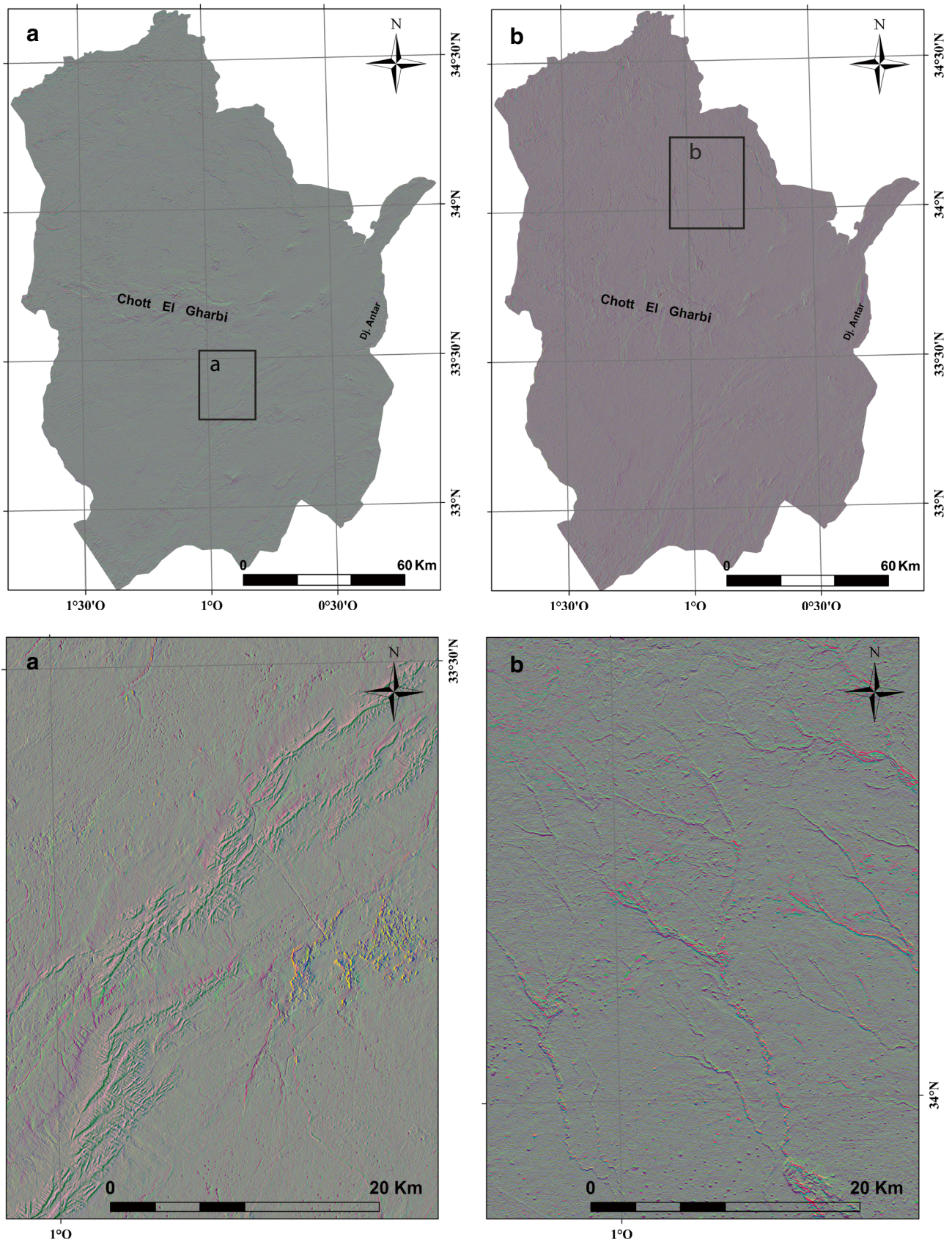


**Fig. 6** Sobel filter applied to the PCA123 following different directions: **a** 0°. **b** 90°. **c** Zoom on the image of sobel filter following the direction 0°. **d** Zoom on the image of sobel filter following the direction 90°

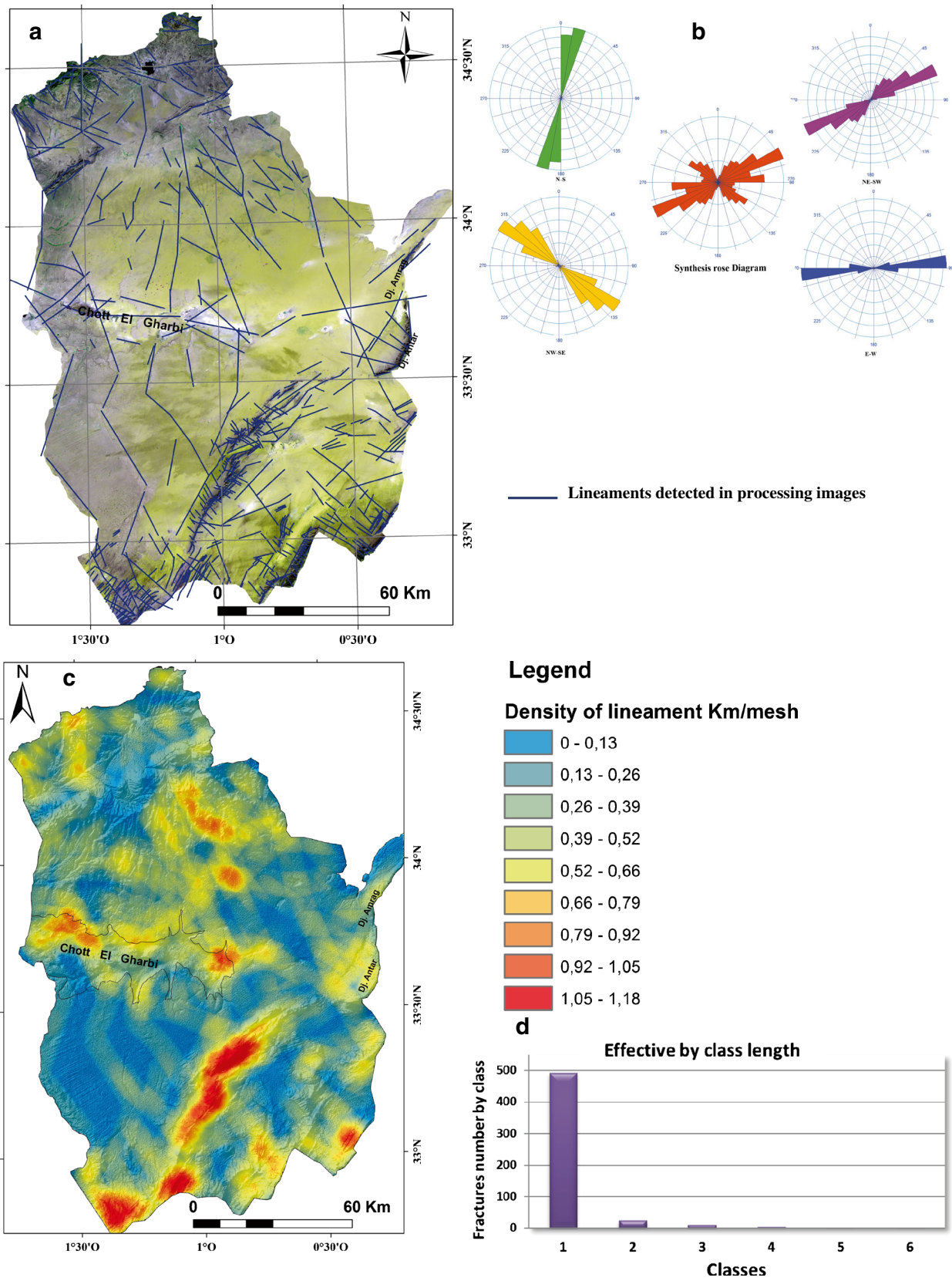


**Fig. 7** **a** Lineaments map derived from satellites images of the study area. **b** Directional rosette of lineaments map derived from satellites images. **c** Density map of fractures of the study area. **d** Lineament histogram grouped in classes according to their lengths

of lineaments NE-SW, NW-SE, N-S (these lineaments are not numerous), and E-W and less important directions ENE-WSW and NNE-SSW.

The NNW-SSE direction corresponding to mega-lineaments crosses diagonally the study area. These lineaments are moved in dextral by the NE-SW lineaments. Another E-W mega-lineament crosses the Chott El Gharbi and seems corresponding to the continuation of the North Atlasic Fault. The NE-SW faults constitute the preferential direction. It corresponds to some well-marked faults in the south and north of the basin (Tlemcen Mounts and Western Saharan Atlas). The NW-SE faults are also visible in the same area as the previous network. They seem formed with the latter a combined system.

The directional rose diagram of the synthesis map (Fig. 7b) shows an important peak in the direction 60°–75° N. So, the lineaments of NE-SW direction are predominant. Three important lineaments in length are in the NNW-SSE direction. They cross diagonally the Chott El Gharbi Basin, with 269, 225, and 129 km in length. Another E-W lineament of 195 km length crosses the depression of the Chott El Gharbi. These two directions (NNW-SSE and E-W directions) of lineaments have a key role in the formation of the Chott, and its water supply.

### Lineament density map

The lineament density map of the study basin is shown in Fig. 7c. This map is produced by applying GIS (Geographic Information System) techniques from lineament map extracted from satellite Landsat 7 images. The area was divided into equal area grids. The number of lineaments in each grid was counted and recorded. The purpose of the lineament density analysis is to calculate frequency of the lineament per unit area (Hassani and Adhab 2014). The fracture density map is expressed in cumulative length of fractures per mesh of 5 × 5 km. The map reveals that the study basin that shows three areas with high lineament density (1.18 km/mesh) occupies the central, south-west, and north-east parts; this high density of discontinuities gives evidence of tectonic movements which have affected the geological formations in the course

**Table 1** Lineament characteristics of the study area

Lineament direction	Number of lineaments	Total length of lineaments (km)	Percentage
NE-SW	300	3121	57%
NW-SE	223	1060	20%
E-W	5	220	4.15%
N-S	10	889	16.80%
Total	537	5290	100%

**Fig. 8** a Geological section AB following the line of hydrogeological surveys (ORGM 2006). b Electric survey at the parametric survey of Bouterkine. c Electric survey at the parametric survey of Sidi Ahmed. d, e Geoelectric sections in the study area (ORGM 2006) (CGG 1974). f Position map of sections

of geological time. This map shows also a low density in most of the study area comparatively to three areas cited above.

### Statistical analysis of lineament networks

The lineament map derived from the satellite images includes 537 structural elements (Table 1), with a total length of about 5290 km; their length varies from 0.53 to 269.93 km with an average length of 9.87 km and a median of 5.23 km. The NE-SW class is the preferential direction. It has a predominant statistical distribution grouping 57% of the total length and 56% of frequencies. The NW-SE fractures include 20% of the total length and 41.41% of the frequencies. The N-S lineaments obtain 16.80% of the total length and 1.86% of frequency, which confirms their kilometeric character length. Finally, the E-W faults obtain 4.15% of the total length and 1.86% of frequencies.

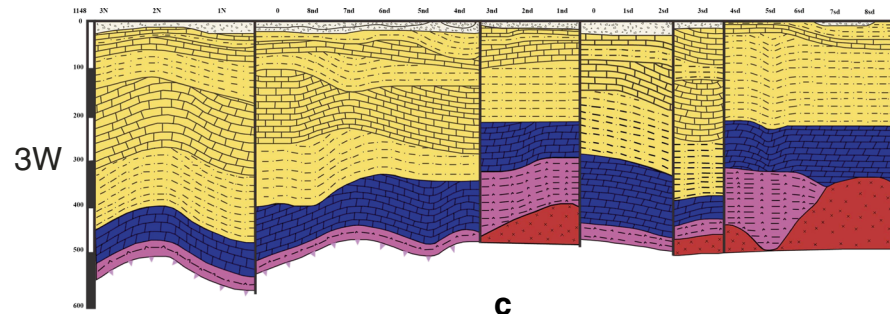
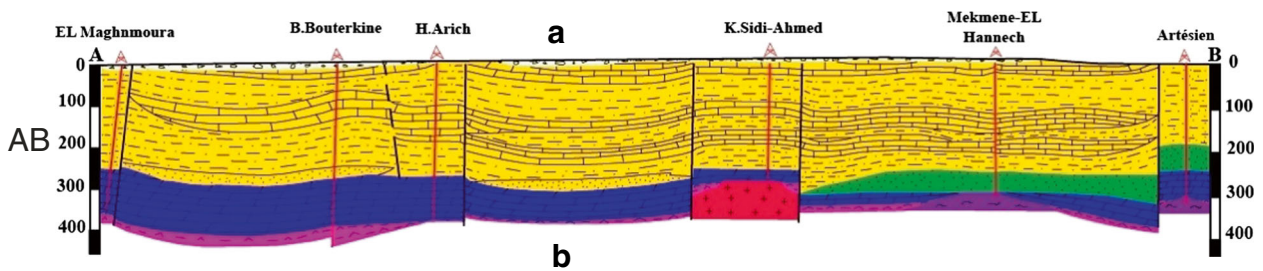
The histogram presented in Fig. 7d shows that more than 493 fractures present less than 30 km in length, and 25 elements have a length between 30 and 100 km. The biggest lineaments whose length exceeds 100 km are therefore the least occurrence. The small lineaments, whose length is between 1 and 30 km, represent more than 95% of the whole tectonic structures.

### Contribution of geophysics data in the lineaments mapping

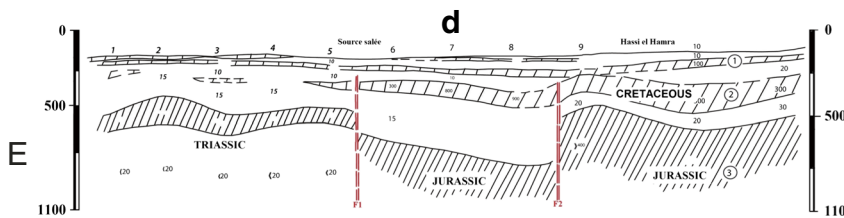
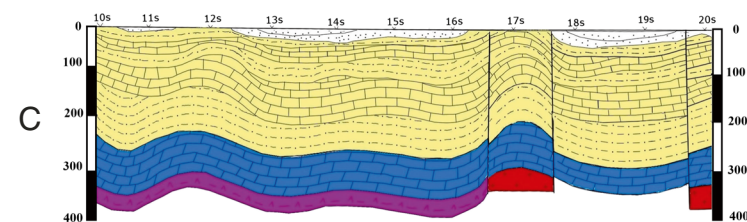
The regional geological section realized by the ORGM (2006) following the line AB through the hydrogeological survey of the Chott El Gharbi Basin (Fig. 8a) shows that the latter (Chott El Gharbi Basin) is affected by major tectonic faults that are divided in several compartments affected by vertical displacement. The section indicates six blocks bounded by faults, in which three of them seem lifted: An oriental block intersects by the Artesian survey, a western block crossed by the Maghbouira survey. Finally a central block which is crossed by the Khoui-Sidi-Ahmed drilling where it note the rise of the substratum by deep faults is noticed (ORGM 2006).

The results of the electrical prospecting realized by the CGG and the ORGM show a multi-directional fracture network affecting all the Jurassic to Quaternary fields (Fig. 8b–d) and confirmed the deep forming of several faults in the Paleozoic basement. These results show the following tectonic characteristics:

- At the depression of the Chott, the faults extend according to NE-SW and NNW-SSE directions. On the west of the

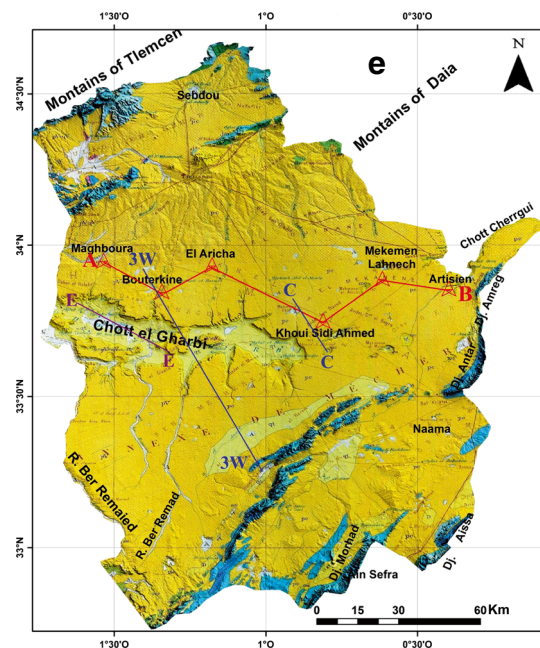


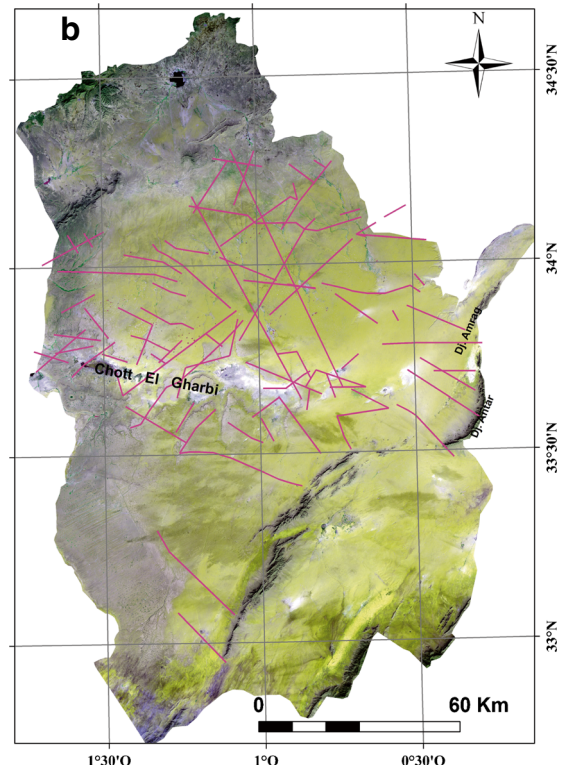
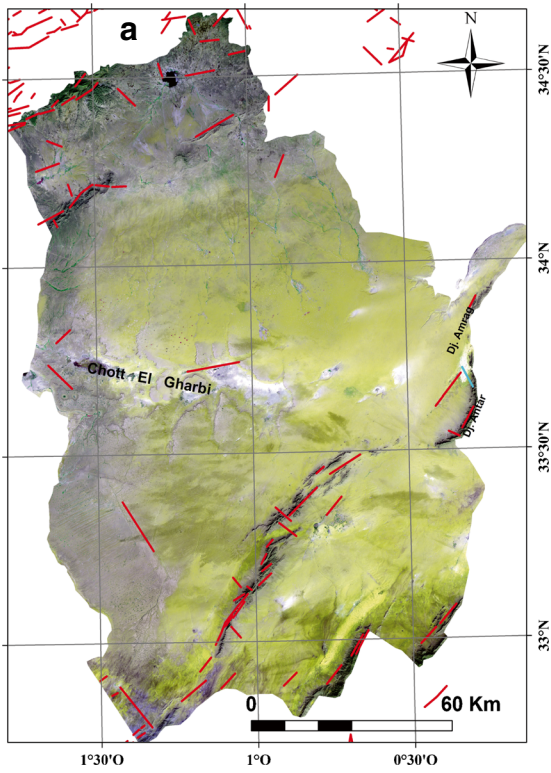
Scale: Vertical 1/50 000  
Horizontal 1/10 000



- Quaternary sediments
- Sandstone and gravels
- Brick sandblaster clay
- White lake limestone
- Gravel and sandstone
- Dolomites
- Marls and clays
- Basic rocks
- Granite
- Hydrogeological survey

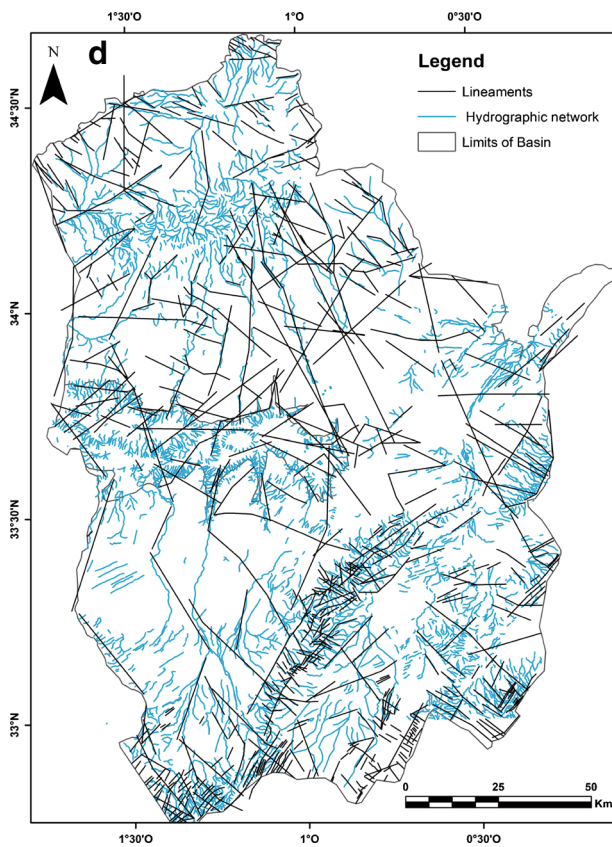
- Major faults according to the aeromagnetic interpretation ORGM, 2006
- Faults according to the geophysical interpretation (CGG, 1974)





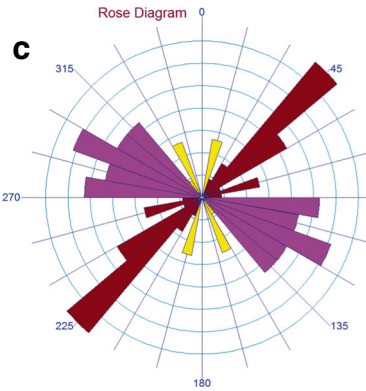
**Legend**

- Lineaments detected by geophysics data
- Lineaments of geological map

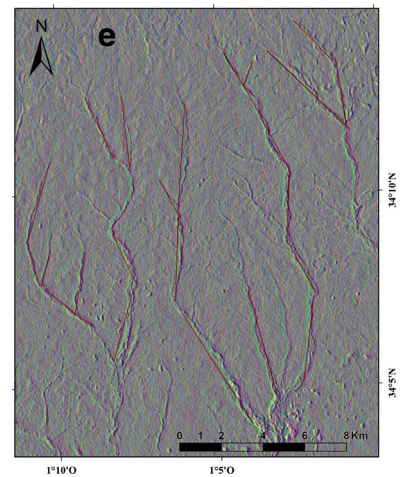


**Legend**

- Lineaments
- Hydrographic network
- Limits of Basin



Statistical Summary	
Calculation Method:	Frequency
Class Interval:	10.0 Degrees
Azimuth Filtering:	Deactivated
Data Type:	Bi-directional
Rotation Amount:	0.0 Degrees
Population:	57
Total Length of All Lineaments:	114.0
Maximum Bin Population:	9.0
Mean Bin Population:	3.8
Standard Deviation of Bin Population:	2.41
Maximum Bin Population (%):	7.89
Mean Bin Population (%):	3.33
Standard Deviation of Bin Population (%):	2.52
Maximum Bin Length:	9.0
Mean Bin Length:	3.8
Standard Deviation of Bin Lengths:	2.41
Maximum Bin Length (%):	7.89
Mean Bin Length (%):	3.33
Standard Deviation of Bin Lengths (%):	2.52
Vector Mean:	193.2 Degrees
Vector Mean:	273.21 Degrees
Confidence Interval:	24.9 Degrees
	(89 Percent)
R-mag:	0.27



◀ **Fig. 9** **a** Lineaments map derived from previous geological map of the study area. **b** Lineaments map derived from geophysical data of the study area. **c** Directional rosette of lineaments map derived from geophysical data. **d e** The relationship between the drainage system and the main tectonic elements and fractures orientation

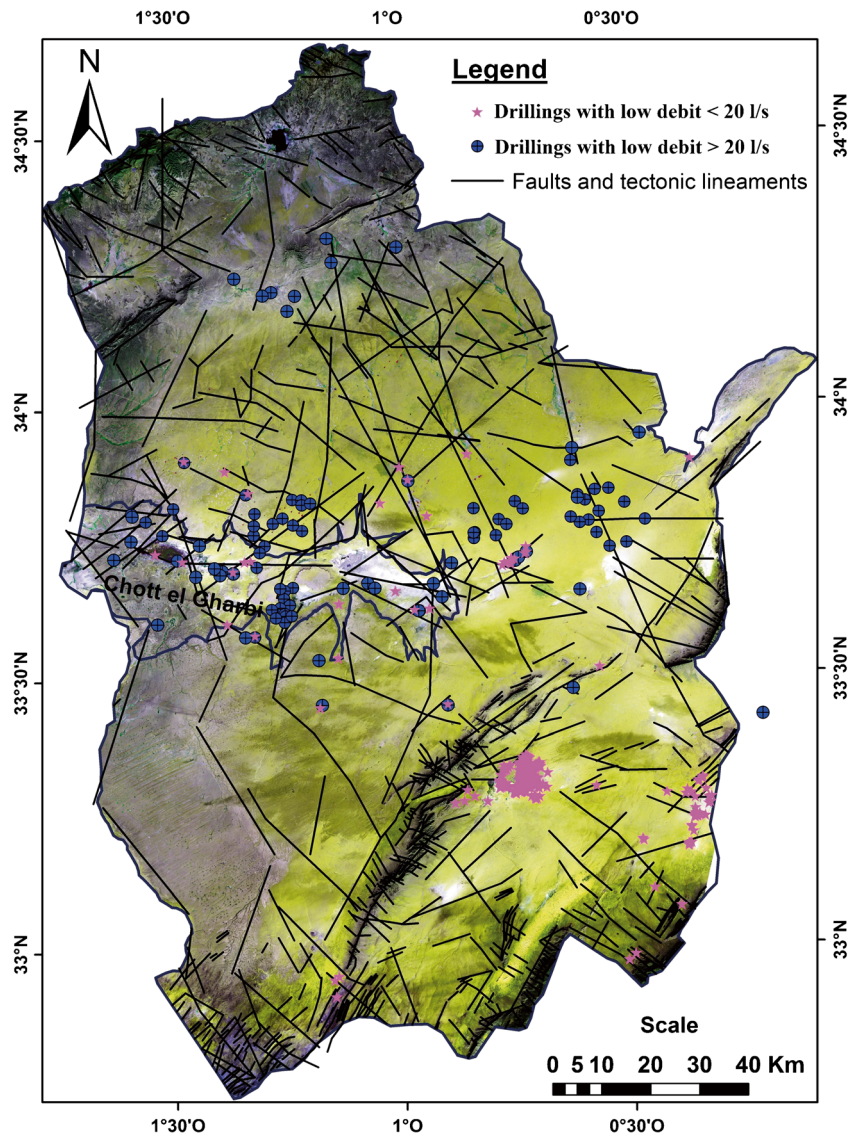
Chott, the NW-SE faults cause subsidence from the Jurassic level until the depths of 400 to 700 m.

- Further east, two other NW-SE parallel faults interrupt the series by raising the Triassic features (Fig. 7e). Three other major accidents of the same direction NW-SE are detected, and a fault which presents setback at Djebel Antar, a last E-W fault which separates Djebel Antar from Djebel Amrag (CGG 1974).
- Longitudinal faults of E-W direction, which could affect the deep Cretaceous and Jurassic features, were also detected by the geophysical methods (CGG 1974).

Therefore, the geophysical methods highlight NE-SW direction faults that are the axis of the synclinal structure. However, this alignment is perturbed by secondary faults. Based on this interpretation, a strong network of main and secondary faults was updated. This set (a strong fault networks) has an important role in the implementation of the Chott, and favorable zones of groundwater accumulation, among these structures the one (a fault) crossing the study area from the N-E to the S-W in the same direction of the principal faults.

In the northwest zone, it is observed the presence of two major (NNW-SSE) faults which have an important role in the circulation of the groundwater. In the south of this area, a complex faults have been highlighted (ORGM 2006).

**Fig. 10** Coupling between synthesis map of lineament and location drillings



## Confrontation of fracture networks with structural geology

Evaluation and validation of the extracted lineaments from digital processing stage of satellite images are essential to judge the efficiency of the method used (Kouamé et al. 1999; Wladis 1999). The confrontation of the lineament map with the existing geological map (Fig. 9a) and lineament map derived by a geophysical investigation (Fig. 9b) shows a big concordance of the identified fractures that extend in the same direction NE-SW, but a large number of faults highlighted on the lineament map derived from the image processing do not appear on the geological map.

## Confrontation of fracture networks with drainage system

The NE-SW direction in the north sector represents the main direction of the drainage network. The abundance of lineaments in this sector compared to the southern sector could be explained by the importance of the drainage network in the northern part (Fig. 9d, e). Comparison of the drainage system and lineament structures has shown that the drainage system of the area is structurally controlled following lineament directions.

## Role of lineaments in underground circulations

The identification of the lineaments role in the groundwater flows is based on the drilling data. The method proposed consists studying the correlation between the drilling flows and their distance to the closest lineament (Koita et al. 2010; Savané 1995).

The total number of drillings is 400, which are differentiated according to two flow classes; the first one corresponding to the drillings whose debit included between 2 and 4 l/s (343 drillings with low debit). The second class corresponds to 59 drillings with debit varying between 25 and 40 l/s (drillings with high debit). This classification (drillings with high and low debit) corresponds to the classification adopted by the committee Inter-State of Hydraulics in West Africa (Koita et al. 2010).

The distances (the shortest straight line perpendicular to the lineament) of each of these drillings to the closest lineament were calculated in order to estimate the evolution of the debit according to the distance between drilling and lineament. Other parameter considered as productivity indices was also taken in the analysis of the debit; it is the depth of the drilling (Koita et al. 2010).

Indeed, the drillings with the high debit have thirty (300) m to forty (400) m in depth, and the depths of the drillings with low debit are between 15 and 40 m.

Coupling of the lineament networks map and the map of spatial repartition of drillings is illustrated by Fig. 10. This map shows that the most of the drillings with high debit are on or near these lineaments. In contrary, the drillings with low debit do not present a particular organization with lineaments. However,

**Table 2** Correlation between the debit drillings and their distance to lineaments

(a) Drillings with high debit (debit > 20 l/s)			
Variables	Distance	Debit	Depth
Distance	1	-0.249	-0.184
Debit	-0.249	1	0.251
Depth	-0.184	0.251	1
(b) Drillings with low debit (debit < 20 l/s)			
Variables	Distance	Debit	Depth
Distance	1	-0.092	-0.148
Debit	-0.092	1	0.394
Depth	-0.148	0.394	1

some zones where drillings have an important debit also present the drillings with low debit. These drillings pick up shallow groundwater of the region and probably have a low hydraulic connection with the major lineaments (Koita et al. 2010).

The analysis of the correlation matrix (Table 2a) between the high debit drillings and their distance to the major lineaments shows that the debit evolves inversely proportional to the distance. The correlation is negative between these two parameters (-0.24). This negative correlation allows asserting that these major regional faults are the seat of an important groundwater circulation, and they have an influence on the hydrodynamic behavior of the region aquifers (Koita et al. 2010; Pistre et al. 1995).

The correlation matrix between the low debit drillings and their distance to the major lineaments (Table 2b) shows the absence of correlation (0.09). This latter confirms that the high potentiality zones are located in the neighborhood of the major discontinuities (Koita et al. 2010).

## Conclusion

The treatment and interpretation of satellite imagery allowed mapping most of the hydrogeological lineaments present in the Chott El Gharbi Basin. The analysis of the fractures networks of this region shows the existence of the dominant orientations of lineaments. The statistical analysis of lineaments indicates preferential directions NE-SW, NW-SE, E-W, and N-S. The NW-SE direction, largest in the north sector, represents the main direction of the drainage network. The study of fracturing intensity revealed that the northern, center, and southern regions of the study area are severely fractured. The validation of these lineaments on the geological map showed the existence of these fractures. Certain lineaments have been validated by geophysical results; these results have confirmed the connection of some lineaments with the deep fractures which are corridors of water circulation. The most productive ones are essentially reservoirs formed by large fracture networks.



Coupling of the lineament network map and the map of spatial repartition of productive drillings allowed the identification of the different types of fractures that could constitute water reservoirs.

The lineament density map shows three areas with high lineament density located in the central, south-west, and north-east parts of the basin.

Comparison of the drainage system and the fractures directions has shown that the drainage system is structurally controlled following lineament directions.

The geophysical prospection in the study area has specified the favorable zone (junction of the fault zones) and the important role of the N-S and E-O fractures.

The identification of the role of lineaments detected in the underground circulation consists of their representation with various drillings on the same map. This final map shows a remarkable correlation between lineaments and drilling flows. This correlation is even more marked in the great lineament E-W which passes the Chott itself and which would be at the origin of its forming, and later at the origin of the aquifers alimentation. These observations confirm the major role of lineaments in the recharge of the deep aquifers of the basin.

**Open Access** This article is distributed under the terms of the Creative Commons Attribution 4.0 International License (<http://creativecommons.org/licenses/by/4.0/>), which permits unrestricted use, distribution, and reproduction in any medium, provided you give appropriate credit to the original author(s) and the source, provide a link to the Creative Commons license, and indicate if changes were made.

## References

- Amadi AN, Olasehinde PI (2010) Application of remote sensing techniques in hydrogeological mapping of parts of Bosso area, Minna, north-Central Nigeria. *Int J Phys Sci Vol 5(9)*:1465–1474
- Auclair D, Biehler J (1967) Étude géologique des hautes plaines oranaises entre Tlemcen et Saida (Geological study of the Oranian High Plains between Tlemcen and Saida). *Publ Serv Carte Géol Alger n. sér, n° 34*, pp 3–45, 4 fig., 6 pl
- Azzaz A (1986) Étude hydrogéologique du Chott el Gharbi. (Hydrogeological study of Chott el Gharbi). Report on the execution of two drillings. National Agency for Hydric Resources ANRH
- Azzaz A (1996) Étude hydrogéologique du Chott el Gharbi. (Hydrogeological study of Chott el Gharbi). Study report, National Agency for Hydric Resources ANRH
- Benabadji N, Bouazza M (2000a) Contribution à une étude bioclimatique de la steppe à *Artemisia herba-alba* Asso dans l'Oranie, Algérie occidentale (contribution to a bioclimatic study of the steppe at *Artemisia Herba-Alba* Asso in Orania (Western Algeria)). *Sécheresse (Paris) 11(2)*:117–123
- Benabadji N, Bouazza M (2000b) Quelques modifications Climatiques Intervenues dans le Sud-ouest de l'Oranie Algérie Occidentale (some climate modifications in southwestern Orania (Western Algeria)), Publication. University of Tlemcen, Algeria
- Benest M (1982) Importance des décrochements sénestres (N-S) et dextres (E-W) dans les Monts de Tlemcen et de Daïa, Algérie Occidentale (Importance of the senescent (N-S) and dexter (E-W) decays in the Tlemcen and Daïa Mountains (Western Algeria)). *Rev Géol Dayn Géogr Phy 23*:345–362
- Benest M (1985) Evolution de la plate-forme de l'Ouest Algérien et du Nord-Est marocain au cours du Jurassique et au début du Crétacé: stratigraphie, milieux de dépôt et dynamique sédimentaire (Evolution of the platform of western Algeria and northeastern Morocco during the Upper Jurassic and early Cretaceous period: stratigraphy, depositional environments and sedimentary dynamics). *Doc Lab Géol Lyon n° 95*, 581 p., 145 fig., 23 pl
- Bensalah M, Adaci M, Mahboubi M, Kazi-Tani O (2005) Les sédiments continentaux d'âge Tertiaire dans les Hautes Plaines oranaises et le tell tlemcenien, Algérie occidentale (continental sediments of tertiary age in the high plains of Oran and the tell Tlemcenaen (western Algeria)). *Soc Geol Esp 18(3–4)*:163–167
- Benzaquen M (1965) Étude stratigraphique préliminaire des formations du bassin de Guercif (preliminary stratigraphic study of the Guercif Basin formation). *Rapp Inédit, Serv Géol Maroc No 30853*, 74 p., 11 figures
- Biémi J (1991) Géologie et réseaux de linéaments, région du bassin versant de la Marahoué, Côte d'Ivoire: cartographie à l'aide des données Landsat-ETM+ et du champ magnétique total. Télédétection et gestion des ressources (Geology and lineaments networks, Marahoué catchment area, Ivory Coast: mapping using Landsat-ETM+ data and the total magnetic field. Remote sensing and resource management). vol vii. Paul Gagnon (éd), Assoc. Q. Teledec, pp 134–145
- Boutaleb S, El Hammichi F, Tabyaoui H, Bouchaou L, Dindane K (2009) Détermination des écoulements préférentiels en zone karstique (Tafrata, Maroc), Apport des données satellitaires SAR ERS-1 et Landsat ETM+ et de la prospection géophysique (determination of the preferential flows in a karstic area (Tafrata, Morocco): contribution of satellite SAR ERS-1 and Landsat EETM++ data and of the geophysical prospection). *J Water Sci 22(3)*:407–419. <https://doi.org/10.7202/037779ar>
- Comet A, Dalloni M, Deleau P, Flandrin J, Gautier M, Gourinard Y, Gousskov N, Laffitte R (1951-1952) Carte Géologique de l'Algérie au 1/500.000 2eme edition (geological map of Algeria to 1/500,000 2nd edition), *Serv Geol Algér*
- Coulibaly L (1996) Interprétation structurale des linéaments par traitement d'image satellitaire: cas des sous provinces d'Abitibi et d'Opatica (Québec) (structural interpretation of lineaments by satellite image processing: the case of the Abitibi and Opatica sub-provinces (Quebec)). Thesis submitted for the degree of Master of Science in Remote Sensing. University of Sherbrooke
- Delteil J, Fenet B, Guardia P, Polvéche J (1971) Géodynamique de l'Algérie occidentale, (geodynamics of western Algeria), *Comptes Rendus somm. Soc Géol Fr 8*:414–417
- Djebaili S (1984) Steppe Algérienne phytosociologie et écologie (Algerian steppe phytosociology and ecology). Office des publications universitaires, Alger 178 p
- Gannouni S, Gabtni H (2015) Structural interpretation of lineaments by satellite image processing (Landsat ETM+) in the region of Zahret Medien (northern Tunisia). *J Geogr Inf Syst 07(02)*:119–127. <https://doi.org/10.4236/jgis.2015.72011>
- Guardia P (1970) Etude structurale du Djebel Fillaoussène et aperçu sur la tectogenèse atlasique dans l'autochtone Oranais, Algérie occidentale (structural study of Djebel Fillaoussène and an overview of Atlasic tectogenesis in the Oranean indigenous (western Algeria)). *Bull Soc Géol Fr 12(7)*:220–225
- Halitim A (1988) Sols des régions arides d'Algérie (soils of arid regions of Algeria). OPU, Alger 384 p
- Hassani M, Adhab SS (2014) Lineament automatic extraction analysis for Galal Badra river basin using Landsat 8 satellite image. *Iraqi J Phys 12(25)*:44–55
- Horton RE (1932) Drainage basin characteristics. *Trans Am Geophys Union 13*:350361

- Israel G, Goldman M, Rabinovich B, Rabinovich M, Issar A (1996) Detections of the water level in fractured phreatic aquifers using nuclear magnetic resonance (NMR) geophysical measurements. *J Appl Geophys* 34:277–282
- Jourda JP (2005) Méthodologie d'application des techniques de Télédétection et des systèmes d'information géographique à l'étude des aquifères fissurés d'Afrique de l'Ouest. Concept de l'hydrotechnique spatiale : cas des zones tests de la Côte d'Ivoire (Methodology of application of remote sensing techniques and geographic information systems to the study of fissured aquifers of West Africa. Concept of Space Hydrotechnics: Case of Ivory Coast Test Areas.), State Doctorate thesis, University of Cocody, p 430
- Jourda JP, Saley MB, Djagoua EV, Kouame KJ, Biemi J, Razack et M (2006) Utilisation des données ETM+ de Landsat et d'un SIG pour l'évaluation du potentiel en eau souterraine dans le milieu fissure précambrien de la région de de Korhogo (nord de la Côte d'Ivoire) : approche par analyse multicritère et test de validation (Use of Landsat ETM+ and GIS data for the assessment of groundwater potential in the Precambrian fissure environment of the Korhogo region (northern Ivory Coast): multicriteria analysis approach and validation test). *Revue de Télédétection*, vol 5, no. 4, pp. 339–357
- Kassou A, Essahlaoui A, Aissa M (2012) Extraction of Structural Lineaments from Satellite Images Landsat 7 ETM+ of Tighza Mining District (Central Morocco). *Int Res J Earth Sci* 4(2): 44–48, ISSN 1995-9044. <https://doi.org/10.5829/idosi.rjes.2012.4.2.1110>
- Koita M, Herve J, Denis R, Kouadio K, Severin P, Issiaka S (2010) Cartographie des accidents régionaux et identification de leur rôle dans l'hydrodynamique souterraine en zone de socle. Cas de la région de dimbokro-bongouanou, cote d'ivoire (Mapping regional accidents and identifying their role in underground hydrodynamics in basement areas. Case of the dimbokro-bongouanou region (Ivory Coast)). *Hydrol Sci J* 55(5):805–820
- Kouamé KF, Gioan P, Biémi J, Affian K (1999) Méthode de cartographie des discontinuités-images satellitaires: Exemple de la région semi-montagneuse à l'ouest de la Côte d'Ivoire (method of cartography of discontinuities-satellite images: example of the semi-mountainous region in western of Ivory Coast). *Télédétection* 2:139–156
- Kouassi GK, Lasm T, Sombo BC, Youan MTA, Baka D, Kouadio KE (2014) Contribution de la géophysique à l'étude structurale et à l'identification des aquifères de fissures dans le Département de Dabakala, Centre-Nord Côte d'Ivoire (Contribution of geophysics in structural study and in identification of fissured aquifers in the department of Dabakala (North Central of Ivory Coast)). *Int J Innov App Stud*. ISSN 2028–9324 8(4):1752–1769
- Kresic N (1994) Remote sensing of tectonic fabric controlling groundwater flow in Dinaric carst. In: Proceedings of the 10th Thematic Conference on Geologic Remote Sensing, 9–12 May 1994, San Antonio, Texas, Environmental Research Institute of Michigan, Ann Arbor, MI, p. 161–167
- Lasm T, Kouamé F, Soro N, Jourda JPR, Biémi J (2004) Analyse géostatistique de la fracturation extraite de l'imagerie spatiale aéroportée et satellitaire. Application à la région de Man-Danané, Ouest de la Côte d'Ivoire (Geostatistical analysis of fracturing from spaceborne and satellite imagery. Application to the region of Man-Danané (West of Ivory Coast)). *Rev Ivoirienne Sci Technol* 5:135–154
- Mahamadou K, Herve J, Denis R, Kouadio K, Severin P, Issiaka S (2010) Cartographie des accidents régionaux et identification de leur rôle dans l'hydrodynamique souterraine en zone de socle. Cas de la région de Dimbokro-Bongouanou (Côte d'Ivoire) (Mapping regional accidents and identifying their role in subterranean hydrodynamics in basement areas. Case of the region of Dimbokro-Bongouanou (Ivory Coast)). *Hydrol Sci J* 55(5):805–820
- Marion A (1987) Introduction aux techniques de traitement d'image (Introduction to image processing techniques). Éditions Eyrolles, Paris 278 p
- Mogaji KA, Aboyeji OS, Omosuyi GO (2011) Mapping of lineaments for groundwater targeting in the basement complex region of Ondo State, Nigeria, using remote sensing and geographic information system (GIS) techniques. *Int. J. Water. Resour. Environ Eng* 3(7): 150–160
- Ndong FB, Ntomba SM, Messi EJ, Okia D, Mvondo JO (2014) Définition structurale des linéaments par traitement d'image satellitaire: cas du massif de Ngovayang, Sud Cameroun (structural definition of lineaments by satellite image processing: case study, the Ngovayang Massif (South Cameroon)). *Afr Sci* 10(3):107–112 ISSN 1813-548X
- N'guessan VH, Saley MB, Wade S, Djagoua EV, Kouamé F, Affian K (2015) Extraction par télédétection et analyse statistique du réseau de fractures, en milieu de socle, dans le département de Sinfra, Centre-Ouest de la Côte d'Ivoire (Extraction by remote sensing and statistical analysis of fracture network, in substratum area, in the department of Sinfra (center-west of Ivory Coast)). *Int. J. Innov. Sci. Res.* ISSN 2351–8014 13(1):225–238
- Office National de Recherche Géologique et Minière (ORGM), (2006) Prospection géophysique à travers le Chott El Gharbi. (National Office of Geological and Mining Geophysical prospection through Chott El Gharbi) ANRH document
- Pistre S, Rives T, Bangoy LM (1995) A new approach for the prediction of unexposed fractured reservoirs: a case study from Millas granite. *Hydrol Sci J* 40(3):351–365. <https://doi.org/10.1080/02626669509491420>
- Savané I (1995) In: Québec (ed) Application de la télédétection à la recherche des eaux souterraines en milieu de socle cristallin: cas d'Odienné, Côte d'Ivoire (Application of remote sensing in search of groundwater of a crystalline basement: case of Odienné, Ivory Coast). AUPELF-UREF, Télédétection et Ressource en eau, Ve journée scientifique de Tunis. Presse de l'Université de Québec, pp 111–120
- Sombo AP, Kouassi F, Sombo B, Kouamé L, Kouassi E (2011) Contribution de la prospection électrique à l'identification et à la caractérisation des aquifères de socle du département de Sikensi, Sud de la Côte d'Ivoire (contribution of electrical prospecting to the identification and characterization of basement aquifers in the department of Sikensi (southern Ivory Coast)), *Eur. J Sci Res* 64(2): 206–219
- Youan MTA, Kouame KF, Koudou A, Adja MG, Baka D, Lasm T, Lasm OD, Jourda JP, Biemi J (2014) Apport de la Cartographie lithostructurale par imagerie satellitaire Landsat 7 à la connaissance des aquifères du socle précambrien de la région de Bondoukou, Nord-Est de la Côte D'ivoire (Contribution of the Lithostructural Mapping By Landsat 7 Imagery To Study the Precambrian Basement Aquifers in Bondoukou Region (Northeast Coast Ivory)). *Int. J. Innov. App. Stud.* ISSN. 2028–9324 7(3):892–910
- Thomas E, Mougouin B, Debeglia N, Perin J (2002) Apport des levés géophysiques aéroportés à la recherche et la protection des ressources en eau: application à la région du Leon, Finistère (The contribution of aerophysical geophysical surveys to the research and protection of water resources: application to the Leon region (Finistère)), Mémoire BRGM/RP-51740-FR, 53 p
- Vouillamoz JM, Legchenko A, Albouy Y, Bakalowicz M, Baltassat JM, Alfares W (2003) Localization of saturated karst aquifer with magnetoresonance sounding and resistivity imagery. *J Ground Water* 41(5):578–587. <https://doi.org/10.1111/j.1745-6584.2003.tb02396.x>

- Wladis D (1999) Automatic lineament detection using digital elevation models with second derivative filters. *Photogramm Eng Remote Sens* 65(4):453–458
- Youan TAM, Lasm T, Jourda JP, Kouam KF, Razack M (2009) Cartographie des accidents géologiques par imagerie satellitaire Landsat-7 ETM+ et analyse des réseaux de fractures du socle précambrien de la région de Bondoukou, nord-est de la Côte d'Ivoire (mapping of geological faults by satellite image Landsat-7 ETM+ and analysis of the network fractures of the Precambrian Basement in Bondoukou Region (Northeast Coast Ivory)). *Téledétection* 8(2):119–135